SANDIA REPORT

SAND2014-18345
Unlimited Release
Printed October 2014

Bistatic SAR: Proof of Concept

David A. Yocky, Neall E. Doren, Terry A. Bacon, Daniel E. Wahl, Paul H. Eichel, Charles V. Jakowatz, Jr., Gilbert G. Delaplain, Dale F. Dubbert, Bertice L. Tise, and Kyle R. White

Prepared by
Sandia National Laboratories
Albuquerque, New Mexico 87185 and Livermore, California 94550

Sandia National Laboratories is a multi-program laboratory managed and operated by Sandia Corporation, a wholly owned subsidiary of Lockheed Martin Corporation, for the U.S. Department of Energy's National Nuclear Security Administration under contract DE-AC04-94AL85000.

Issued by Sandia National Laboratories, operated for the United States Department of Energy by Sandia Corporation.

Available to DOE and DOE contractors from
U.S. Department of Energy
Office of Scientific and Technical Information
P.O. Box 62
Oak Ridge, TN 37831

Telephone: (865) 576-8401
Facsimile: (865) 576-5728
E-Mail: reports@adonis.osti.gov
Online ordering: http://www.osti.gov/bridge

Available to the public from
U.S. Department of Commerce
National Technical Information Service
5285 Port Royal Rd.
Springfield, VA 22161

Telephone: (800) 553-6847
Facsimile: (703) 605-6900
E-Mail: orders@ntis.fedworld.gov
Online order: http://www.ntis.gov/help/ordermethods.asp?loc=7-4-0#online

SAND2014-18345
Unlimited Release
Printed October 2014

Bistatic SAR: Proof of Concept

David A. Yocky, Neall E. Doren, Terry A. Bacon, Daniel E. Wahl, Paul H. Eichel, and Charles V. Jakowatz, Jr.
Signal & Image Processing Technologies

Gilbert G. Delaplain
Intelligence, Surveillance, & Reconnaissance (ISR) Analysis & Applications

Dale F. Dubbert
ISR EM & Sensor Technologies

Bertice L. Tice
ISR Real Time Processing

Kyle R. White
Structures & Mechanisms

Sandia National Laboratories
P.O. Box 5800
Albuquerque, New Mexico 87185-MS1207

Abstract

Typical synthetic aperture RADAR (SAR) imaging employs a co-located RADAR transmitter and receiver. Bistatic SAR imaging separates the transmitter and receiver locations. A bistatic SAR configuration allows for the transmitter and receiver(s) to be in a variety of geometric alignments. Sandia National Laboratories (SNL) / New Mexico proposed the deployment of a ground-based RADAR receiver. This RADAR receiver was coupled with the capability of digitizing and recording the signal collected. SNL proposed the possibility of creating an image of targets the illuminating SAR observes. This document describes the developed hardware, software, bistatic SAR configuration, and its deployment to test the concept of a ground-based bistatic SAR. In the proof-of-concept experiments herein, the RADAR transmitter will be a commercial SAR satellite and the RADAR receiver will be deployed at ground level, observing and capturing RADAR ground/targets illuminated by the satellite system.

ACKNOWLEDGMENTS

This work would not have been possible without the support of many people from several organizations. The authors wish to express their gratitude to the National Nuclear Security Administration, Defense Nuclear Nonproliferation Research and Development (DNN R&D). Our team would like to thank our program leader, Veraun Chipman from NSTec for his help and support of our efforts. This work was done by Sandia National Laboratories under award number DE-AC52-06NA25

Our team would like to thank SNL employees and contractors Robert Abbott, Sean Hollister, and Samuel Bolin for their support and work on this effort. Also, thanks to Cathy Snelson-Gerlicher, formerly of NSTec now at Los Alamos National Laboratory, and Robert White from NSTec for their help and support of our efforts.

CONTENTS

FIGURES

TABLES

NOMENCLATURE

A	Amps
AC	alternating current
ADC	analog-to-digital converter
API	application programming interface
BRRS	bistatic RADAR receiving system
C	Celsius
DC	direct current
FPGA	field-programmable gate array
GPS	global positioning system
Hz	Hertz
I/O	input/output
ISR	Intelligence, Surveillance, & Reconnaissance
LED	light emitting diode
MPPT	Maximum Power Point Tracking
NSTec	National Securities Technologies
PC	personal computer
PCS	power control subsystem
PWM	pulse width modulation
RADAR	radio detection and ranging
RAID	redundant array of independent disks
RAS	recording automation subsystem
RF	radio frequency
RMS	root mean square
SAR	synthetic aperture RADAR
SNL	Sandia National Laboratories
TCP	transmission control protocol
TLE	two line element
UDP	user datagram protocol
USB	universal serial bus
UTC	coordinated universal time
V	volts
VAC	volts alternating current
W	Watt

1. INTRODUCTION

Sandia National Laboratories (SNL) has developed airborne RADARs and signal processing methods for synthetic aperture RADAR (SAR) systems since the late 1980's. SNL's Signal and Image Processing Technologies Group has played a major role in developing SAR imaging and exploitation techniques [1, 2, 3, 4]. SNL's Airborne Intelligence, Surveillance, & Reconnaissance (ISR) Systems Group designs and deploys state-of-the-art SAR systems and algorithms that have been and are still being used for U.S. government and civilian applications [5, 6, 7, 8, 9].

1.1. Background

While typical SAR imaging employs a co-located RADAR transmitter and receiver, bistatic SAR imaging separates the transmitter and receiver locations. A bistatic SAR configuration allows for the transmitter and receiver(s) to be in a variety of geometric alignments. For example, if the transmitter illuminates the ground from behind the receiver position, the scattered signal from the target is captured as it travels back, toward the receiver's position. This is called backscatter. If the transmitter illuminates the ground from a location in front of the receiver, the scattering signal is called "forward scatter". Side scattering positions fill the rest of possible collection geometries.

SNL proposes the deployment of a ground-based RADAR receiver. If this RADAR receiver is coupled with the capability of digitizing and recording the signal collected, one could capture SAR radiation illuminating targets of interest. The irradiating SAR would not know the ground-based receiver's location, thus the SAR signal is passively and covertly captured. If the transmitted and reflected signals are captured from the illuminating SAR, SNL proposes the possibility of creating an image of targets the illuminating SAR observes.

The bistatic RADAR receiving system consists of two RADAR receivers (horn antennas). The first receiver will be pointed skyward to capture the direct signal from the illuminating RADAR. The second receiver will be directed toward the ground region of interest to capture the targets illuminated by the transmitting RADAR. These RADAR signals will be captured by the antennas, digitized by hardware, and stored on a hard drive for later analysis and image formation.

This document describes the developed hardware, software, bistatic SAR configuration, and its deployment to test the concept of a ground-based bistatic SAR. In the proof-of-concept experiments herein, the RADAR transmitter will be a commercial SAR satellite and the RADAR receiver will be deployed at ground level, observing and capturing RADAR ground/targets illuminated by the satellite system.

1.2. Objectives

The objectives of the proposed research are to:

1. Capture SAR illumination from various sources using a ground-based RADAR receiver.

2. Produce imagery from the captured SAR illumination.

The first research step was to construct hardware and develop software that could fulfill the above objectives. The second step in this research was to test the hardware/software by deploying it locally, i.e., at Kirtland Air Force Base (AFB). The third research step was to deploy the bistatic SAR ensemble to Nevada National Security Site (NNSS) to bistatically capture activity there. The Source Physics Experiment (SPE) IV explosive event was selected as this activity.

This proof of concept is reported in the following. First, the hardware and software needed for a ground-based bistatic SAR is described. Secondly, operational considerations are covered. Thirdly, experiments devised to test the equipment are described with their results, culminating in an experiment at NNSS to bracket the SPE IV experiment which was scheduled for 10:30 Pacific Daylight Time, August 15, 2013.

2. HARDWARE AND SOFTWARE: FIRST ITERATION

2.1. Overview

The reflected signals of a SAR collection is a convolution of the transmitted waveform and the reflection function of the targets illuminated [1]. Convolving the return signal with a conjugated transmitted signal deconvolves the transmitted waveform leaving the reflection function of the targets illuminated. Therefore, passively collecting an active SAR collection to make a SAR image requires two signals:

1. The transmitted signal before it scatters off the earth.

2. The reflected signal after the transmitted signal scatters off the earth.

The following documents our first iteration on hardware and software to capture signals from a SAR sensor and to make an image.

2.2. Hardware and Software Components

Given the objectives above, two signals from a SAR sensor require capture and conversion into electrical signals. These electrical signals should be amplified and digitized to provide digital signals to process. The following sections discuss how the SAR electromagnetic radiation is transduced into a digital signal appropriate for signal processing and SAR image formation.

2.1.1. RADAR Antennas

A RADAR transmits electromagnetic waves created by applying a pulsed, oscillating, radio-frequency (RF) current and voltage to an antenna. The frequency and bandwidth of the transmitted signal are controlled by electronics that excite the transmitting antenna. In a reciprocal way, a RADAR antenna irradiated by electromagnetic energy from the transmitter will convert that energy into a proportional RF current and voltage at the antenna output. A typical receiver design also requires a high-gain, low-noise amplifier (LNA) and associated components located as closely as possible to the antenna. Collectively these components are often referred to as the “RF front end”.

Pyramidal horn antennas designed for X-band, 8 to 12 GHz, were used for the direct- and reflected-energy antennas. Figure 1 shows the block diagram for a horn antenna and the RF front end.

2.1.2. Receiver Base Station

A 25-foot coaxial cable allows the direct- and reflected-energy antennas to be positioned away from received-signal base station. Note this gives less signal loss than that designed with the 50-foot cables in Figure 1. The base station consists of a down-converter, a personal computer (PC), a digitizer, a redundant array of independent disks (RAID), and an uninterruptable power supply (UPS).

2.1.2.1. Down-converter

Both the direct and reflected X-band RADAR signals enter the down-converter where they undergo a two-stage bandpass filtering and frequency down-conversion from a center frequency of 9.6 GHz to a 400 MHz intermediate frequency (IF) output signal. The down-converter also contains RF attenuators controllable by front panel switches or universal serial bus (USB) remote control. These switches facilitate adjusting both direct and reflected signal path amplitudes independently to a signal level appropriate for proper digitization by the analog-to-digital converter (ADC). Appendix A contains a block diagram of the down-converter.

The down-converter front panel has two light-emitting diode (LED) bar graph indicators that display the amplitude of the signal received by the reflected- and direct-energy antennas respectively. SNL ISR designed and built the down-converter.

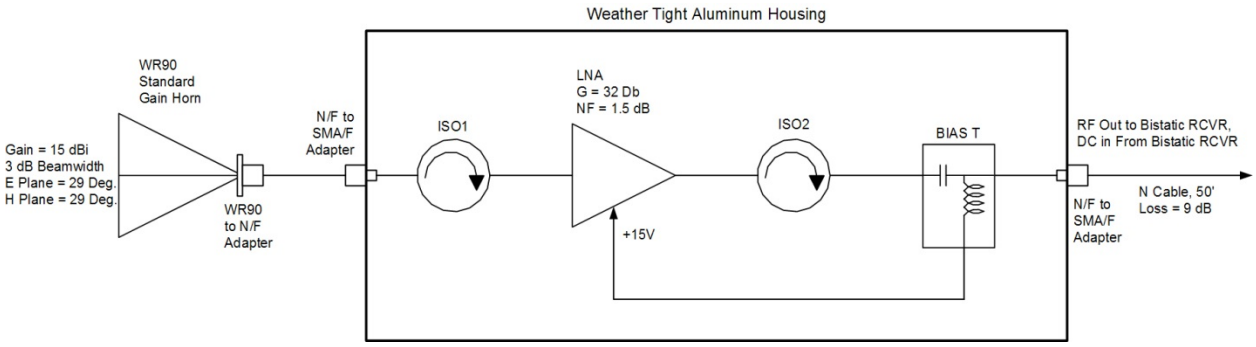

Figure 1. Block diagram of a receive horn antenna, isolators, a low-noise amplifier (LNA), and a power source.

2.1.2.2. Digitizer

SNL chose the Pentek Talon® RTR 2749 as the recording system. It is a ruggedized system that can record high-bandwidth signals under conditions of vibration and shock. The Pentek® digitizer has a 4U, 19-inch, rack-mountable PC server chassis. In dual-channel mode, it has a maximum sample rate of 1.6 GHz. It employs an ADC with 12 and 8-bit packing modes. The real-time sustained recording rate maximum is 3200 MB/sec. The digitized data can be stored on

7.68 TB of solid-state disk (SSD) storage in the form of a new technology file system (NTFS) RAID disk array. Figure 2 shows the front of the Pentek Talon® and the RAID. Figure 3 shows the rear of the Pentek® chassis. The data stored on the RAID can be extracted via USB 2.0 or 3.0 removable disks. The USB ports are located on the front and back panels of the PC as shown in Figure 2 and Figure 3.

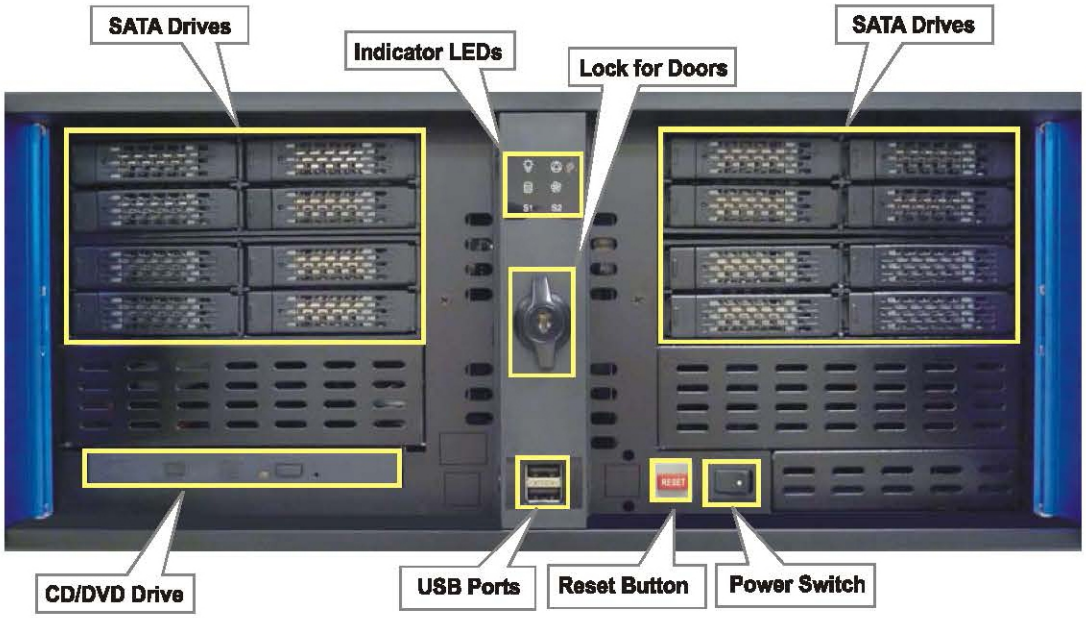

Figure 2. Pentek Talon® front with panels open.

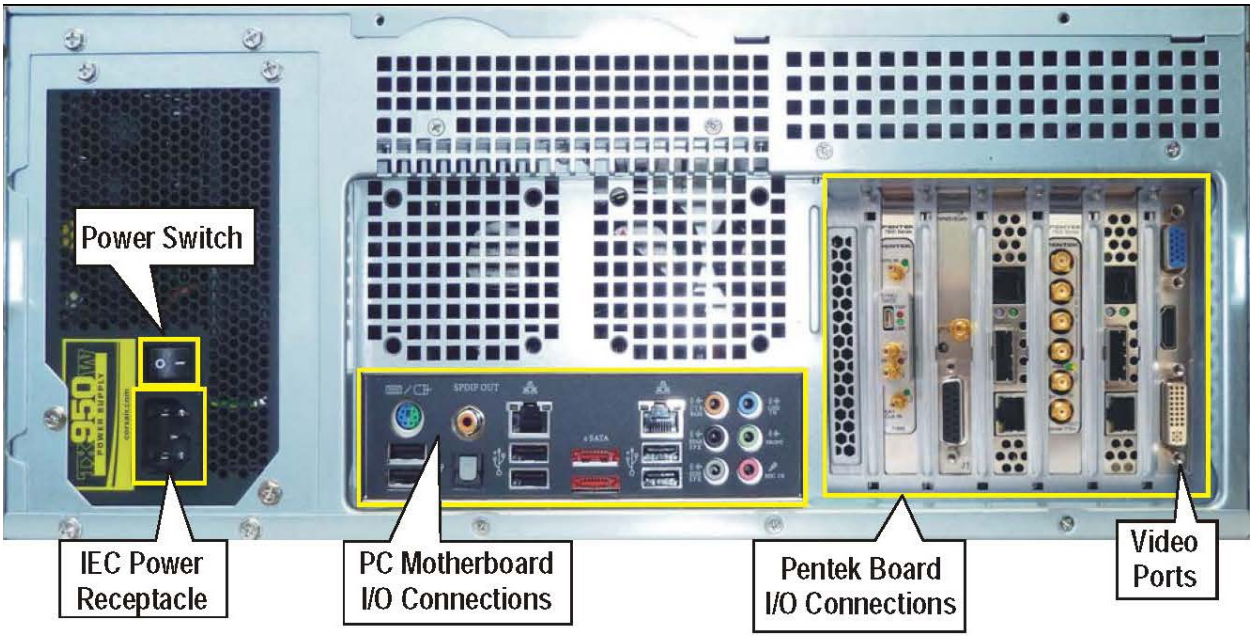

Figure 3. Pentek® rear chassis.

The digitizer interface is through a Windows® 7 workstation with an Intel® Core™ 7 processor. The Pentek® has a graphical user interface (GUI) with Signal View analysis tool. This tool allows the real-time signal levels to be viewed graphically on the computer screen. Figure 4 shows the Signal View display. The digitizer also has a GUI allowing for manual and automatic recording. Here the user defines file names and can manually press record or set a time and duration for recording data. The recorded data files have headers that include time stamping and recording parameters. There is an option to include global positioning system (GPS) time and position stamping.

2.1.2.3. UPS

The electrical supply is through a 120 VAC, 20 amp power cord into the UPS. An APC® Smart UPS, 2200VA, 120V provides an uninterruptable power source if the electrical source fails or wavers. The UPS is capable of a power load of 500 W for about 40 minutes, and 1900 W for 5 minutes. The base station uses less than 500 W, so it can be powered for over 40 minutes without an electrical source provided the UPS is fully charged.

2.1.2.4. Ruggedized Rack

A shock-resistant rack was purchased to transport the base station. The rack dimensions are: 27□ x 35□ x 33□ with attachable 3.5□ diameter casters on the bottom. The rack has handles and latches on the side for tie-down. Figure 5 shows the final configuration of the base station components fielded in an air-conditioned van.

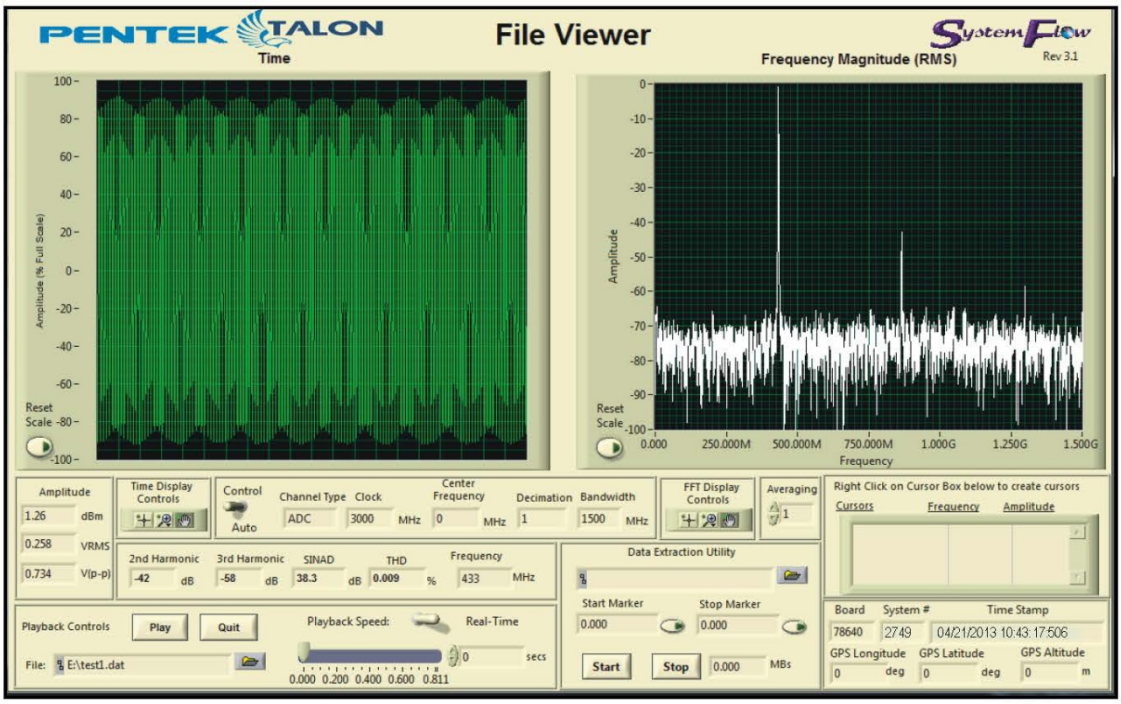

Figure 4. Pentek® Signal View GUI.

Figure 5. Final configuration of the bistatic receiver base station in the ruggedized rack. The UPS is the bottom location in the rack. The Pentek® RAID and PC ensemble is directly above it. In the third position is the SNL down-converter. The keyboard and terminal occupy the top position in the rack.

3. EXPERIMENTAL VERIFICATION: FIRST ITERATION

3.1 Overview

To verify the validity of the overall idea and the realization of the hardware/software to acquire SAR signals, field tests were conducted on Kirtland AFB, Albuquerque, NM, on which SNL resides. Since the bistatic receiver is ground-based, it is essential to find a "perch", a site where the direct-signal antenna is unimpeded by tall obstacles that might block the line-of-sight to the illuminator. The perch should also be elevated with line-of-sight to the ground targets of interest, and distant from the targets to provide a wide field of view. The following reports the illuminators, the "perch", the targets, and the results for preliminary collections on Kirtland AFB.

3.2 SAR Illuminators

Several X-band SARs orbit the earth. Tasking these satellites through various entities provides SAR illuminators for which the collection geometry, the time of collection, and the possible signal power levels are known. Knowing these parameters beforehand, the efficacy of the bistatic SAR receiver can be tested.

3.2.1 COSMO-SkyMed

The X-band Italian SAR called COSMO-SkyMed (CSK) operates at 9.6 GHz center frequency, and a variable bandwidth from 180 to 400 MHz. It is funded by the Italian government ministry of defense, Ministero della Difesa (MDD) and ministry of education, universities, and research, Ministero dell'Istruzione, dell'Università, e della Ricerca, (MIUR), and operated by Agenzia Spaziale Italiana (ASI). Four CSK satellites are in low-earth (LEO), sun-synchronous orbits at approximately 620 km above the earth, with an orbit inclination of 97.9° and an orbit cycle of 15 days. Together, the four satellites are able to repeat an image of a target within 24 hours. A typical image covers a 10 km by 10 km area.

3.2.2 TerraSAR-X

TerraSAR-X (TSX) is a dual-use (commercial and military) X-band SAR with a 9.65 GHz center frequency operated by the public-private partnership between Deutsches Zentrum für Luft- and Raumfahrt (DLR) and Astrium/European Aeronautic Defence and Space Company (EADS). TSX is a single satellite in a LEO, sun-synchronous orbit of 514 km with an orbit inclination of 97.4° and an orbit repeat of 11 days. It has a maximum bandwidth of 300 MHz. A typical image covers a 5 km by 10 km area.

Table 1. Table of commercial SAR collections for the proof-of-concept field experiments.

Satellite	Mode	Date and Time (UTC)	Azimuth Angle (degrees)	Look Angle (degrees)	Target
CSK-2	Enhanced Spotlight	11Jun13, 00:46:10	278.08	48.18	TAGC
CSK-3	Enhanced Spotlight	12Jun13, 00:46:16	278.08	48.19	TAGC
CSK-4	Enhanced Spotlight	15Jun13, 00:46:17	278.08	48.16	TAGC
TSX	High-Resolution Spotlight Mode	01Aug13 13:15:52	280.49	26.86	TAGC

3.3 Deployment

Manzano Mountain on Kirtland AFB provides a large relief above the plains that gradually slope to the Rio Grande. Figure 6 shows a Google Earth® image of Kirtland AFB with a pin at the deployment site on Manzano Mountain and the target, Tijeras Arroyo Golf Course (TAGC) and its club house. The deployment point is at 35° 01□ 22.9□ N, 106° 29□ 14.8□ W with a relief of 340 m and a stand-off distance of 3.68 km from TAGC. CSK and TSX can illuminate from east-to-west in a descending orbital pass, or from west-to-east in an ascending orbital pass. Manzano Mountain offers backscatter (descending orbit) and forward-scatter (ascending orbit) bistatic capture geometries. Backscatter geometry will produce an image closest to the monostatic SAR image sensed by the illuminator.

Two four-wheel-drive vehicles climbed the unmaintained dirt road to a shoulder on Manzano Mountain overlooking the TAGC. The vehicles carried the base station, a gas-powered generator, the two RADAR antennas, and a GPS antenna, along with five Sandians. The site was selected because of the abrupt drop-off toward the plain below, clear sight of the TAGC clubhouse, and no obstructions to block the SAR satellite signals. The base station was powered by a 3 kVA Honda gas-powered generator with a 20 amp socket. The antennas are deployed on sturdy tripods equipped with inclinometers and compasses. The direct- and reflected-energy antennas were deployed, and their locations measured by a hand-held GPS receiver. The antennas were connected to the base station, and their functioning was checked by a battery-powered microwave source and horn on a tripod irradiating each antenna from approximately 5

meters distance while monitoring the signal displayed on the Pentek® Signal View GUI via the PC monitor. Procedures were followed to assure the correct attenuations and record time were input into the Pentek® GUI and the recorder was armed and readied for the known overflight time. Figure 7 through Figure 10 show the deployment of the direct- and reflected-energy antenna, and cables to the base station, the power generator, and the line-of-sight of the reflected-energy antenna.

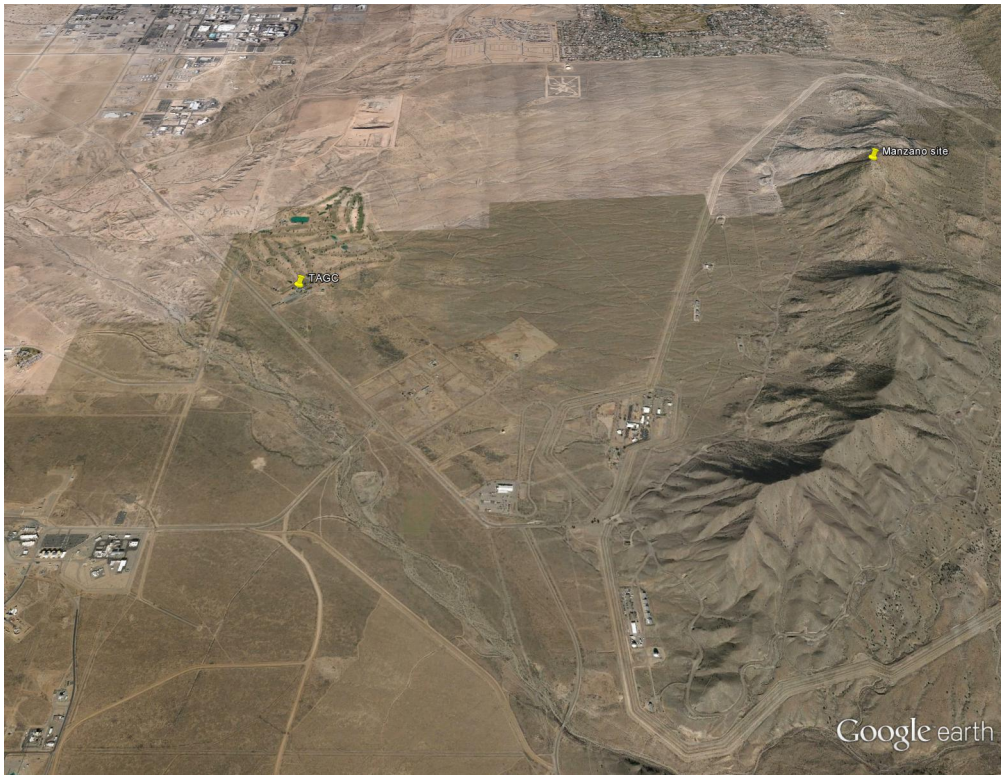

Figure 6. Google Earth® optical image of Manzano Mountain and Tijeras Arroyo Golf Course on Kirtland AFB.

Figure 7. Manzano Mountain antennas set up. The direct-energy antenna is in the background. The reflected-energy antenna is in the foreground.

Figure 8. Rear panel of the base station. The gold box is the down-converter. The black back-panel is the Pentek® digitizer. The white-looking cables are the antennas coaxial cables. A gray cable is seen below them. This is the GPS antenna input for clock time stamps and PC reference time.

Figure 9. The rear of a 4-wheel vehicle holding the base station. Two antenna cables, one GPS cable, and a black power cable enter the air-conditioned vehicle through the back window. The gas-powered electric generator is in the foreground.

3.4 Captured Signal and SAR Imagery

Three CSK RADAR collections were made on June 10, 11, and 14, 2013. From these first collections, it was important to analyze the signal levels of both the direct and reflected energy. The digitized signals should not saturate the ADC such that signal levels were lost. Also, the digitized signal should be distinguishable from noise, or the system would not be sensitive enough to discern between signal and noise. If the signals are of the correct level, and knowing the position of the illuminator, the signals can be processed and formed into an image.

3.4.1 Signal Levels

Using the digitized data, the reflected- and direct-energy signals can be analyzed for the number of bits used to capture the signals. The ADC was selected to 8 bit mode. Figure 11 shows the voltage levels of the direct energy signal. Each peak is a waveform pulse from the CSK satellite. Given the maximum voltage of 0.3972 volts (V), the number of bits used to digitize the direct-energy signal is between 5 and 6 bits. There is no saturation in this signal. Figure 12 shows the voltage levels of the reflected-energy signal. Each pulse is the reflected CSK pulse received at the reflected-energy antenna. The reflected signal uses the same digital levels as the direct energy. There is definite signal seen for the pulses. Note that the "constant" signal below 0.02 V is the thermal noise of the antenna system and any other background noise from the scene.

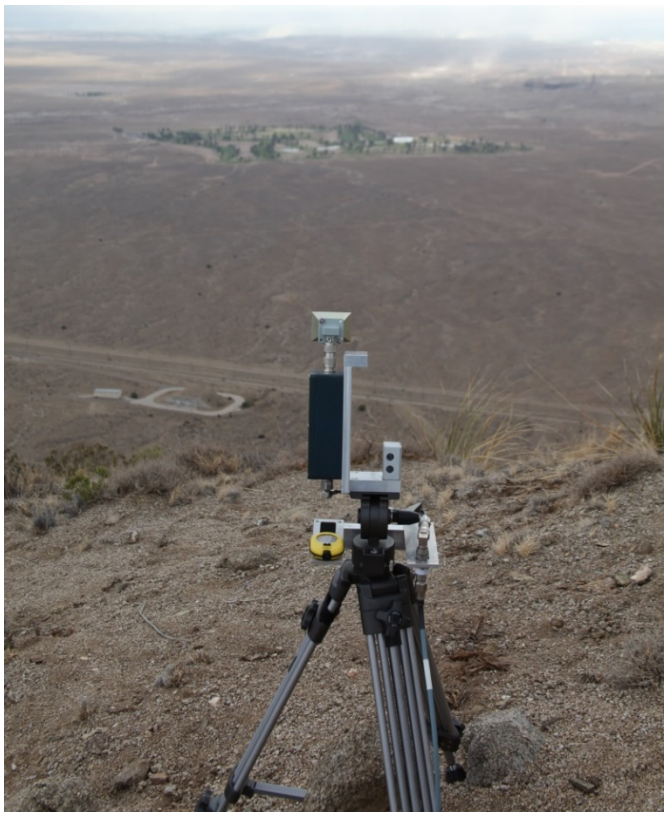

Figure 10. Looking down the reflected antenna toward the TAGC in the distance.

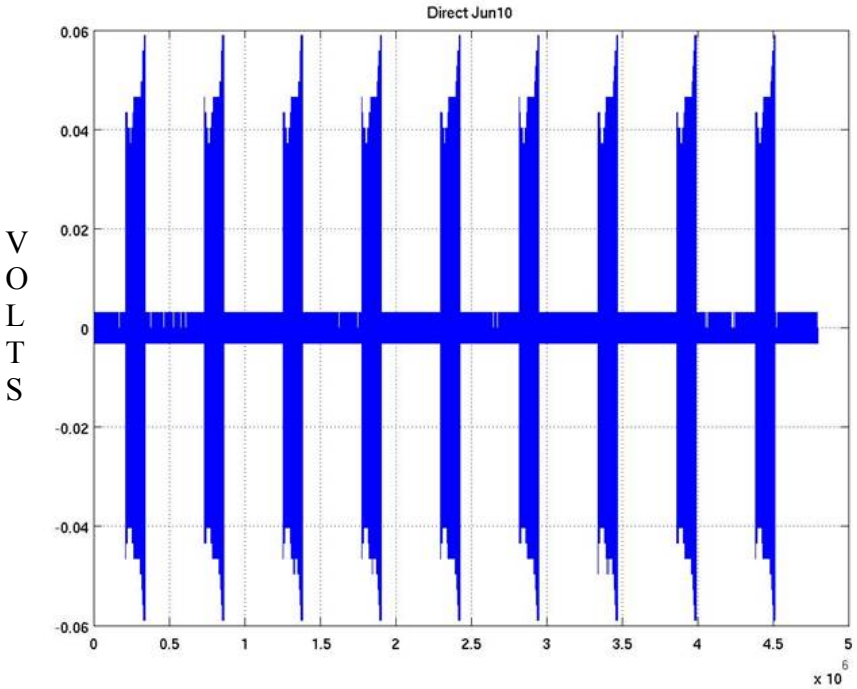

Figure 11. Plot of direct energy digitized signal from June 10, 2013 CSK collect. Signal uses 5 to 6 bits out of 8 bits.

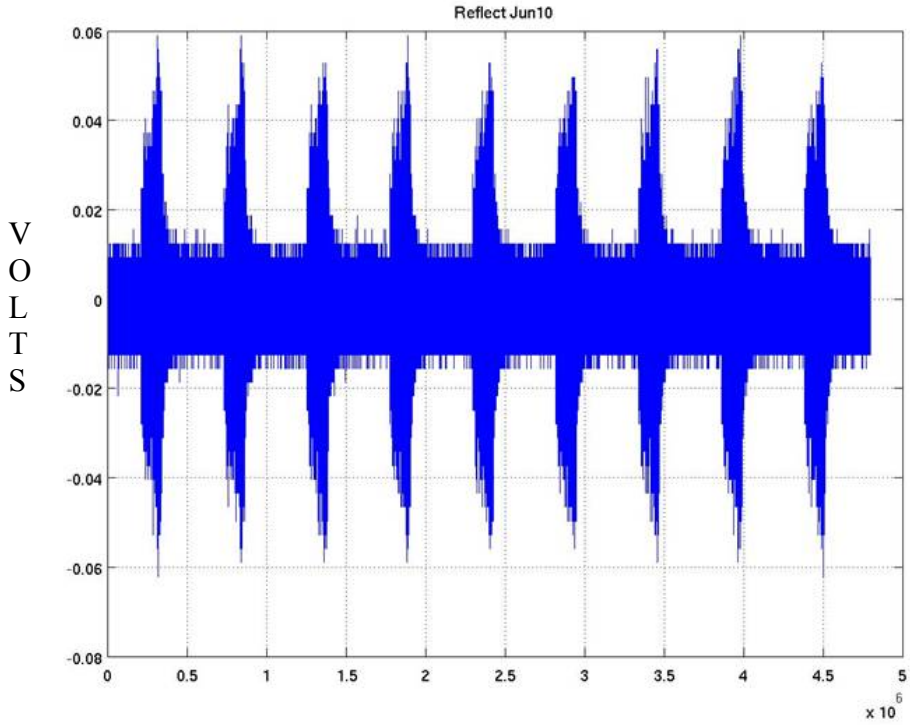

Figure 12. Plot of digitized reflected energy during June 10, 2013 CSK collection which uses between 5 and 6 bits out of 8 bits of dynamic range.

3.4.2 Data manipulation

The direct energy channel provides the timing of the incoming energy in both channels. It also supplies characteristics of the impinging RF radiation. This knowledge helps arrange the reflected energy into a phase history and provide the waveform to deconvolve the illuminating waveform and recover the target reflectivity. A two-line element (TLE) file provides the ephemeris for the SAR sensor. TLEs for most satellites are readily available on the internet. The process of estimating the waveform, data assembly, and image formation will be covered at another time.

3.4.3 Image formation

The CSK collection was pseudo-spot-light-mode. A popular spot-light mode image formation algorithm is polar format algorithm (PFA) [1]. This algorithm will produce an image if the complex phase history is assembled coherently, and the ephemeris correctly predicts the satellite position during the collection. The PFA image of the June 10, 2013 CSK collected at 18:46:10 Mountain Daylight Time (MDT) is shown in Figure 13. This is a range-Doppler image with range being up and down the page. The bright spot at the top of the image is the position of the reflected-energy antenna. It is very bright due to targets reflecting close to the antenna, and possibly energy leaking in the back-lobe of the antenna. A triangular SAR image is below this

with approximately a 30° angle, the field-of-view of the reflected-energy antenna. The targets closer to the reflected-energy antenna are brighter because of proximity to the antenna. The targets farther from the antenna exhibit energy decrease because the reflected power drops as the inverse of the target to antenna distance squared. The extent of the SAR image is approximately 8200 m from the antenna to far-range reconstructed targets.

Figure 14 shows a close-up of the TAGC. The trees, the fairways, and water hazard are apparent in the image. The Tijeras Arroyo is to the left of the golf course. Note that roads are not straight, but curved. This is due to wavefront/range-curvature, which is not corrected using PFA. Though maybe not apparent in this close-up of the scene center, the range-curvature effect can cause defocussing of SAR targets farther from scene center.

Figure 15 presents a geo-located image of the entire reconstructed bistatic CSK image. This geo-located data was put on a latitude/longitude grid. Note there may be some signal leaking into the antenna's back lobe. The reflections behind the reflected-energy antenna are due to ambiguities in the data very near the antenna position.

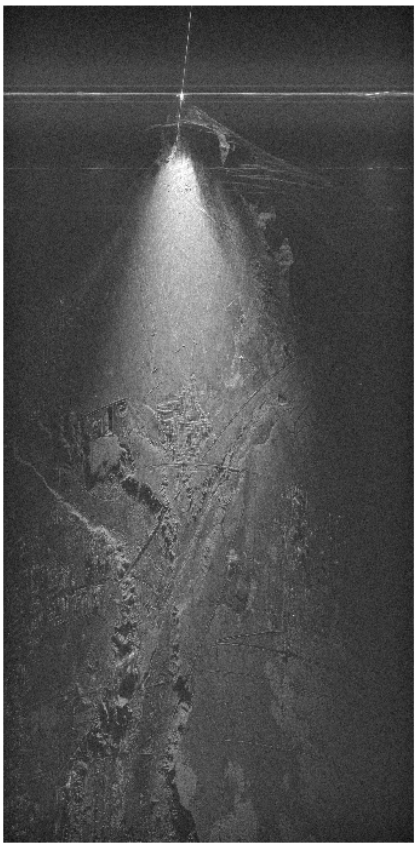

Figure 13. Radar coordinates bistatic SAR image of the TAGC from Manzano Mountain on June 10, 2013, 18:46:10 MDT.

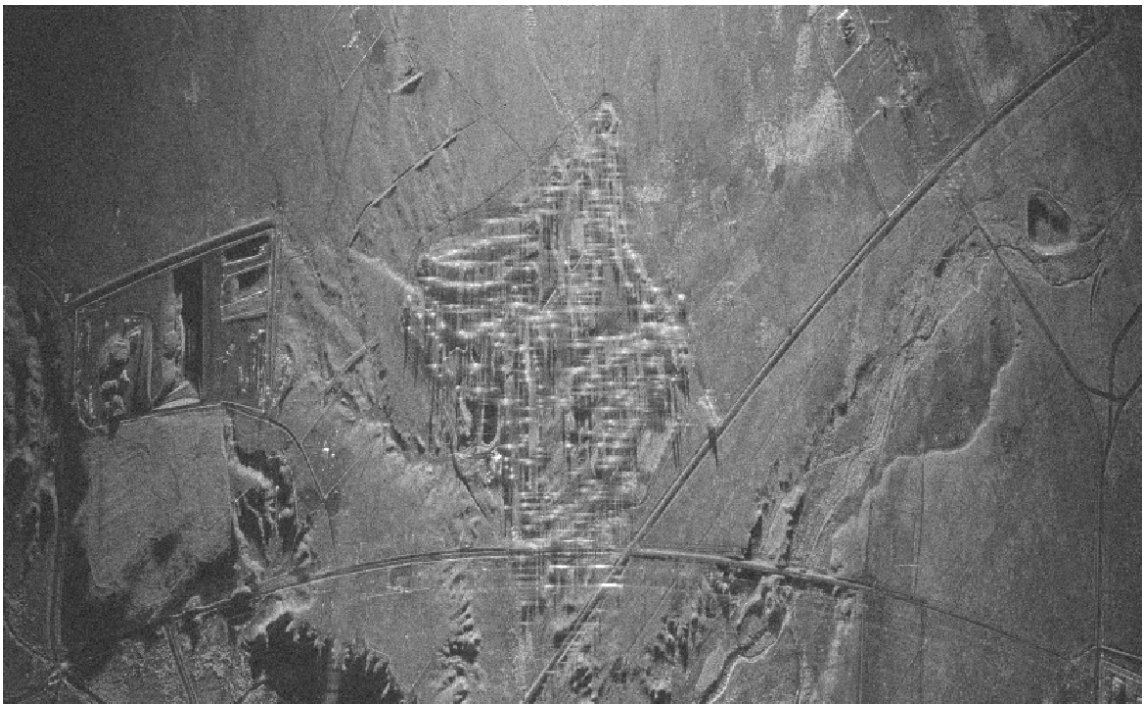

Figure 14. Close-up of the TAGC. Note the roads are curved due to range curvature using PFA.

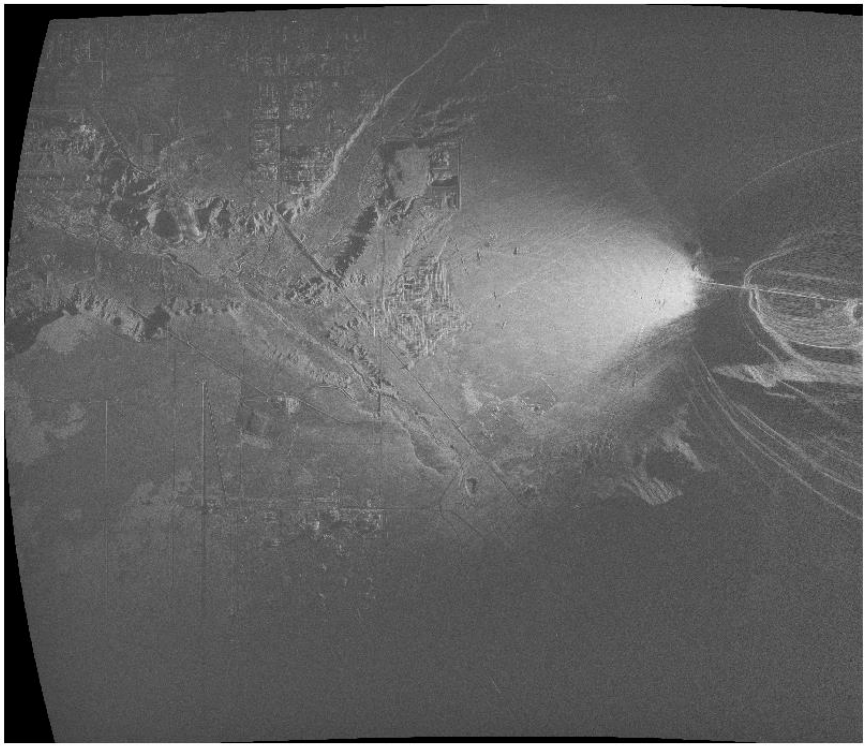

Figure 15. Geo-located bistatic SAR image of TAGC captured on June 10, 2013. This image is on a latitude/longitude grid.

Figure 16 shows a close-up of geo-located imagery of TAGC from CSK on June 10, 2013. The image on the left is the geo-located bistatic CSK imagery captured from Manzano Mountain. The image on the right is the geo-located monostatic CSK image collected at the satellite. Note that the target reflectivity and shadows are quite different in the bistatic and monostatic images. The trees at the TAGC are smeared because they are moving respect to the 5.6° elevation angle in the bistatic, yet they appear focused and not moving with respect to the monostatic, 42.8° elevation angle image.

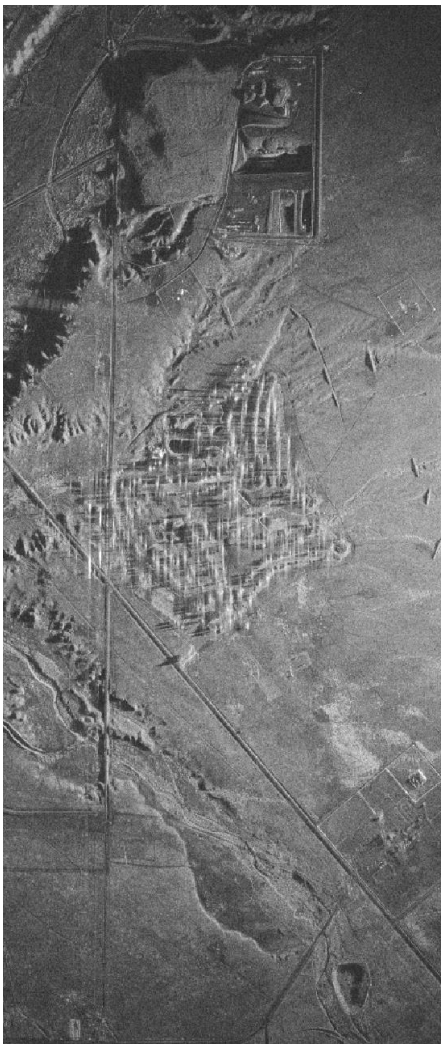

Figure 16. The image on the left is the bistatic SAR, geo-located image of TAGC. The image on the right is the monostatic CSK SAR image from the commercial imagery vender. Note the differences in shadows. The bistatic elevation angle is about 5.6° and the monostatic elevation is 42.8°, making the bistatic shadows more pronounced. The target reflectances are quite different in some cases.

4. EXPERIMENTAL VERIFICATION: SECOND ITERATION

4.1. Hardware Upgrades

During the first excursions up Manzano Mountain, the antennas experienced high amounts of vibration. This loosened a couple of mounting screws on one antenna, causing the antenna horn to move with respect to the front end box. Modifications were made to the antennas assemblies to assure the horn could not move, and the screws were secured with locking fluid. Also, two hard golf-bag-carrying cases where acquired to place the two RADAR antennas on their tripods, the RADAR source on its tripod, and the GPS antenna and its tripod.

The bright reflectance seen in the SAR imagery at the reflected-energy antenna contained sidelobes that radiate far into the image. The first-order characteristics of the antenna were explored. Figure 17 presents a plot of the antenna sensitivity as a function of location. Note there is some back-lobe sensitivity. Nevertheless, most of the sensitivity occurs in the 30° forward looking direction. Reduction of near-range reflections could reduce the signal at the reflected-energy location.

A flexible, magnetically loaded, silicone rubber tape was placed on the tips of the reflected-energy antenna horn to reduce the near-field scattering into the antenna. This product was made by Emerson & Cuming Microwave Products called ECCOSORB® MCS. Other options are currently being pursued.

4.2. SAR Illuminator and Deployment

Instead of CSK as the illuminator, SNL tasked TSX to illuminate TAGC as documented in Table 1. With the new antenna cases, and ruggedized antenna modifications, the direct- and reflected-energy antennas were deployed on Manzano Mountain at the same locations as in June 2013.

4.3. Captured Signal and SAR Imagery

One TSX RADAR collection occurred on August 1, 2013. Since TSX is a different SAR, SNL needed to analyze the signal levels of both the direct and reflected energy. Just as with CSK, the digitized signals should not saturate the analog-to-digital converter (ADC) such that signal levels were lost. Also, the digitized signal should be distinguishable from noise, or the system would not be sensitive enough to discern between signal and noise. If the signals are of the correct level, knowing the position of the illuminator the signals can be processed and formed into an image. The attenuation level for the TSX was lower than that used for CSK.

4.3.1. Signal Levels

Using the digitized data, the reflected- and direct-energy signals can be analyzed for the number of bits used to capture the signals. The ADC was placed in 8 bit mode. Figure 18 presents the voltage levels of the direct-energy signal. Each peak is a waveform pulse from the TSX satellite. Given the maximum voltage of 0.3972 V, the number of bits used to digitize the direct energy signal is between 6 and 7 bits. This signal is not saturated. Figure 19 shows the voltage levels of the reflected-energy signal. Each pulse is the reflected TSX pulse received at the reflected-energy antenna. The reflected signal uses the same digital levels as the direct energy. There is definite signal seen in the pulses. Note that the "constant" signal below 0.02 V is the thermal noise of the antenna system and any other background noise from the scene.

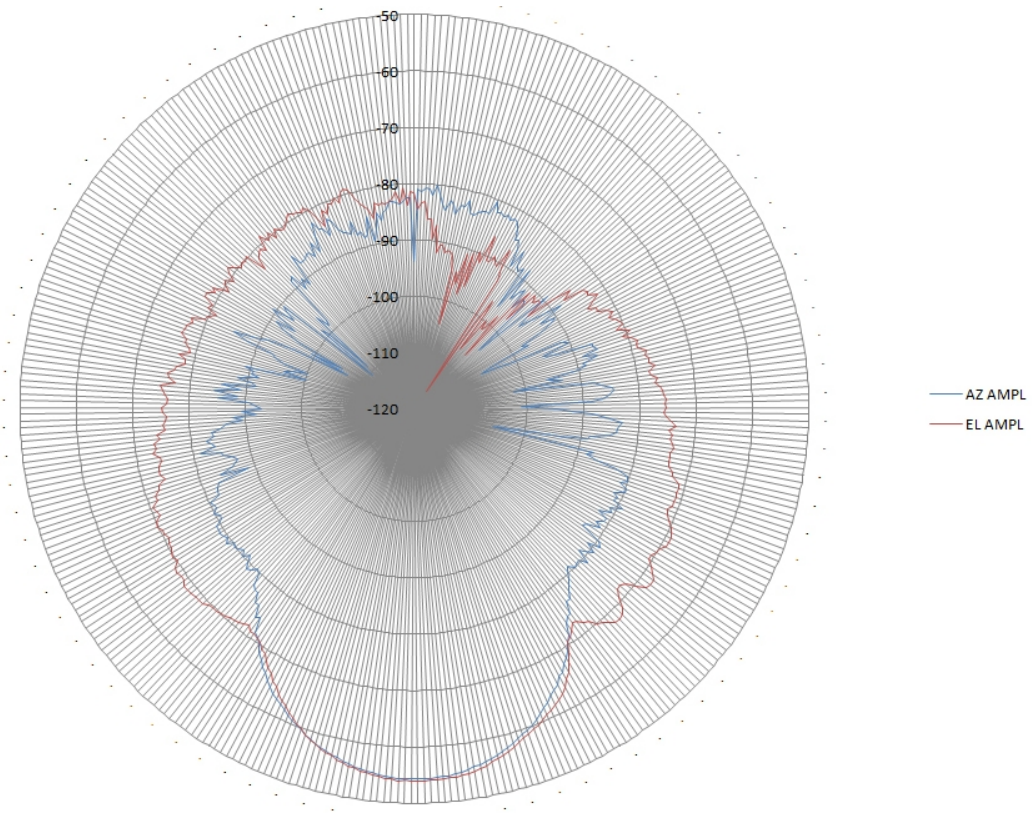

Figure 17. Reflected-energy antenna signal sensitivity characteristics as a function of azimuth and elevation angles.

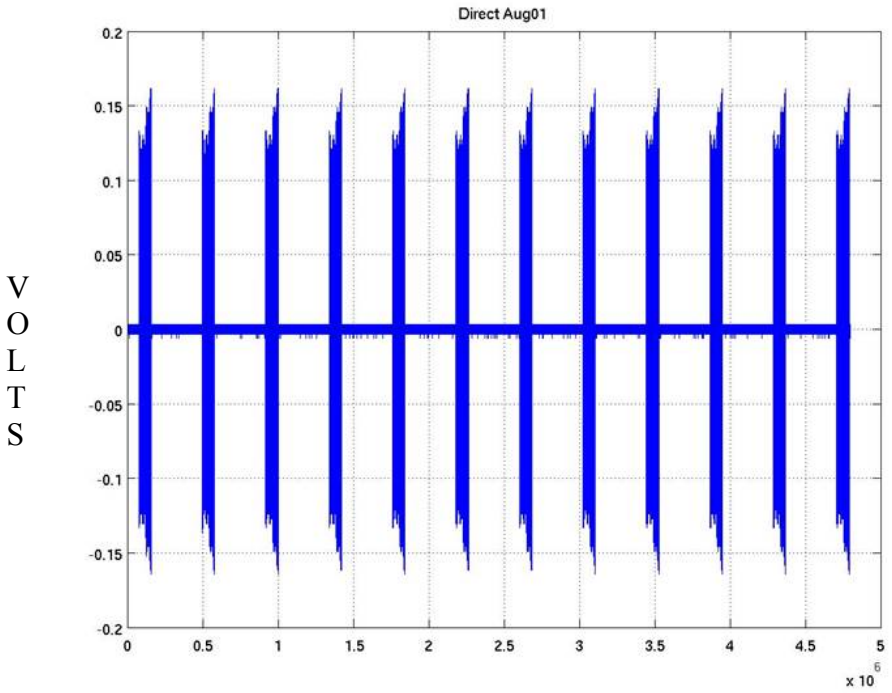

Figure 18. Plot of direct energy digitized signal from August 1, 2013 TSX collect. Signal uses 6 to 7 bits out of 8 bits.

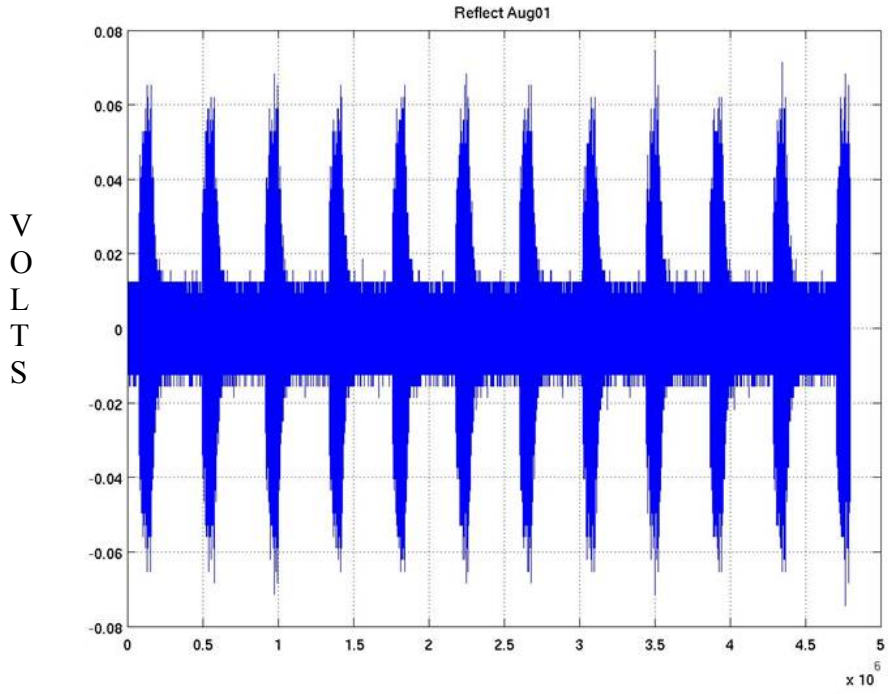

Figure 19. Plot of digitized reflected energy during August 1, 2013 TSX collection which uses between 5 and 6 bits out of 8 bits of dynamic range.

4.3.2. Image formation

The TSX collection was pseudo-spot-light-mode. The polar format algorithm image of the August 1, 2013 TSX collected at 07:15:52 MDT is shown in Figure 20. This is a range-Doppler image with range being up and down the page. Overall, the image resembles the CSK images captured in June. The extent of the SAR image is approximately 9500 km from the antenna to far-range reconstructed targets.

Figure 21 presents a geo-located image of the entire reconstructed bistatic TSX image. This geo-located data was put on a latitude/longitude grid. Figure 22 shows a close-up of geo-located imagery of TAGC from TSX on August 1, 2013. The image on the left is the geo-located bistatic TSX imagery captured from Manzano Mountain. The image on the right is the geo-located monostatic TSX image captured at the satellite. Note that the target reflectivity and shadows are quite different in the bistatic and monostatic images. Compared to the CSK bistatic imagery in Figure 16, the motion of the trees is negligible in the TSX bistatic image.

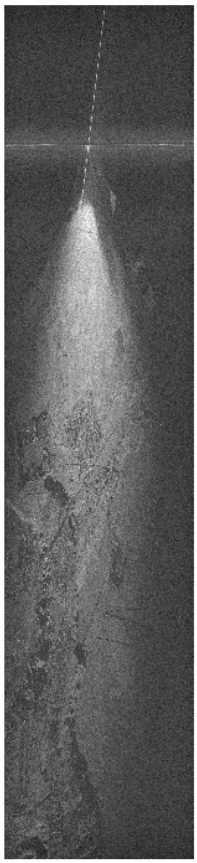

Figure 20. TSX Bistatic image of TAGC captured on August 1, 2013, 07:15:52 MDT. Image created using PFA.

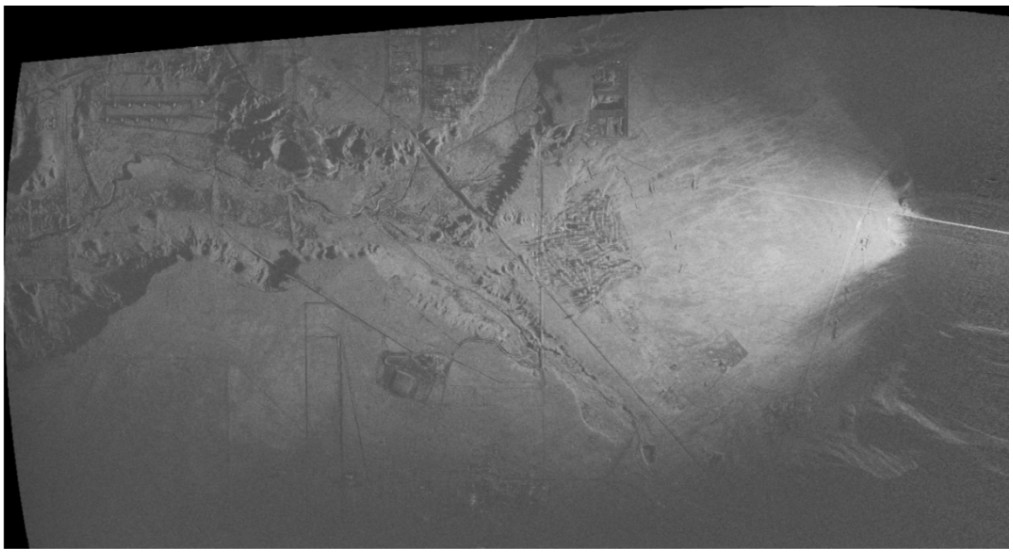

Figure 21. Geo-located TSX bistatic SAR imagery captured August 1, 2013 from Manzano Mountain

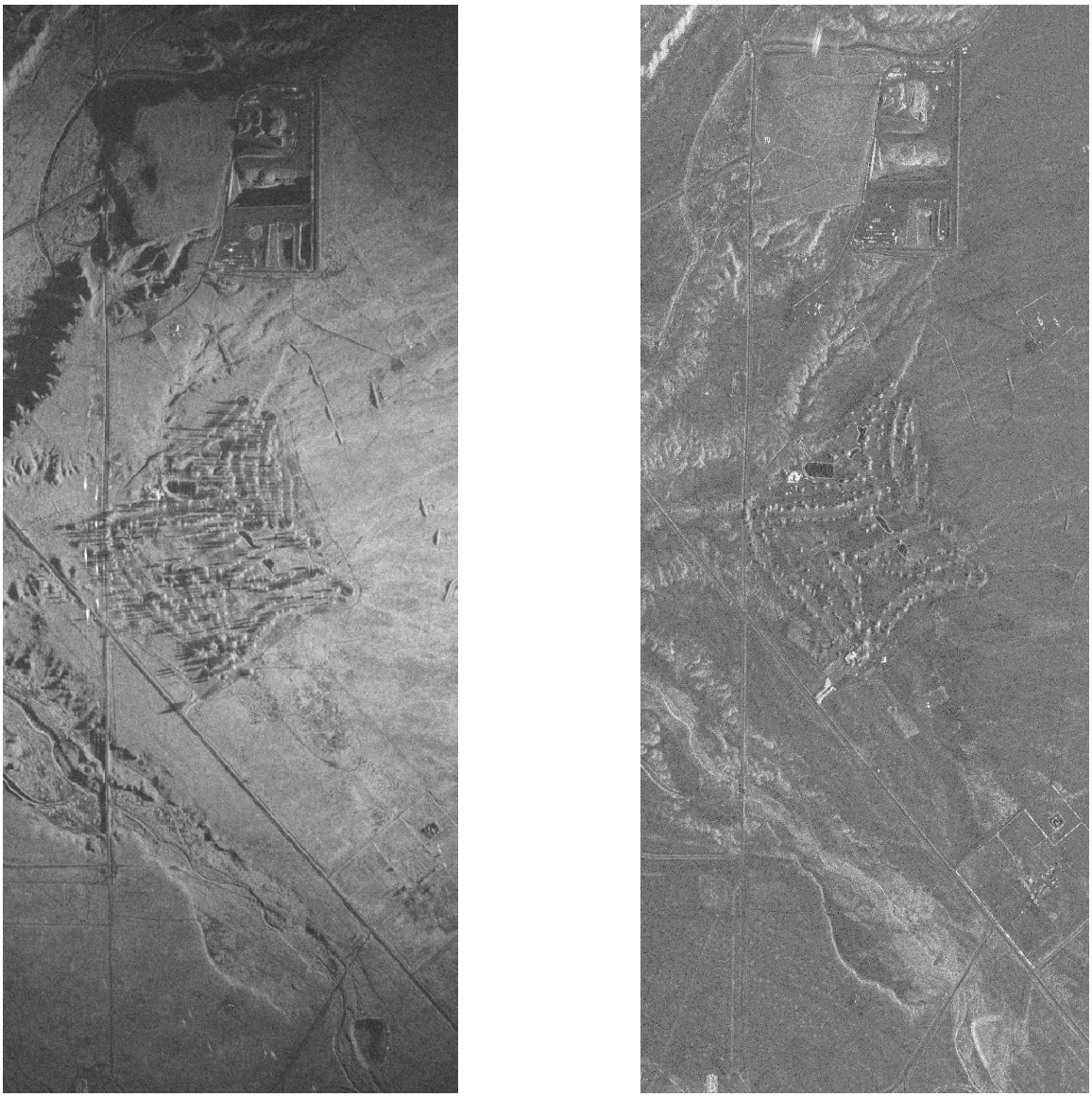

Figure 22. The left image is a close up of TAGC from the geo-located bistatic TSX SAR imagery. The right image is a close up of TAGC from the geo-located monostatic TSX SAR image.

5. NEVADA NATIONAL SECURITY SITE TEST

5.1. Overview

Sandians travelled to Nevada National Security Site (NNSS) in April and in July, 2013, teaming with National Security Technologies (NSTec) personnel to visit prospective bistatic SAR test sites. Three NNSS sites were visited in April: SPE site, Monastery, and Check Point Pass. Motorola and Skull Mountain were inspected from a distance. In July, two sites were visited: SPE site and Little Skull Mountain West. A site overlooking over the SPE site was selected to monitor the activity related with the Source Physics Experiment (SPE) series of underground conventional explosives tests. On August 15, 2013, the underground explosives test SPE IV was scheduled. Appendix B documents SNL's tasking of NSTec.

5.2. NNSS Site

A flat drill pad has been created at 37° 13□ 16.8□ N, 116° 03□ 38.8□ W at NNSS. At this site, three underground conventional explosive tests have been conducted. The site is instrumented to monitor seismic, acoustic, and other signals pertinent to characterizing the explosions. The site is in the foothills at the north-most extent of Yucca Flat. It is surrounded by mountainous terrain to the east, north, and west.

To the north-northeast of the SPE pad, an unmaintained mining road rises to an overlook of the SPE site. It is approximately 1530 m away with a relief of 160 m above the SPE site at coordinates 37° 14□ 03.6□ N, 116° 03□ 22.6□ W. This overlook provides a side-scattering geometry for bistatic signal collection, but it was the only site that gave relief above the SPE site, a good stand-off distance, and a line-of-site to monitor SPE activities. Also, commercial SAR imagery was permitted to be collected over the SPE site. Figure 23 shows a Google Earth® optical image of SPE and the overlook.

5.3. Transportation

A four-wheel-drive, high-clearance van was provided by SNL's Geophysics & Atmospheric Sciences Department. The base-station rack, antenna ensembles, and generator were loaded into the van and secured. This van served as transportation to NNSS. It also traversed the unmaintained road to the SPE overlook. Sandians drove the van from Albuquerque to Las Vegas, and then to Mercury in preparation for deployment on August 15, 2013.

5.4. SAR illuminator and Deployment

CSK and TSX were tasked to illuminate the SPE site as documented in Table 2. With the new antenna cases, and ruggedized antenna modification, the direct- and reflected-energy antennas were deployed at the SPE overlook. NSTec employees helped drive the four-wheel-drive van to SPE overlook. Another four-wheel-drive vehicle was needed to transport other personnel to the overlook. Figure 24 shows the van, early testing of signals received from the RF source antenna, and the SPE site in the distance. Figure 25 shows the position of the reflected-energy antenna and the GPS antenna. Figure 26 shows the base station setup in the van.

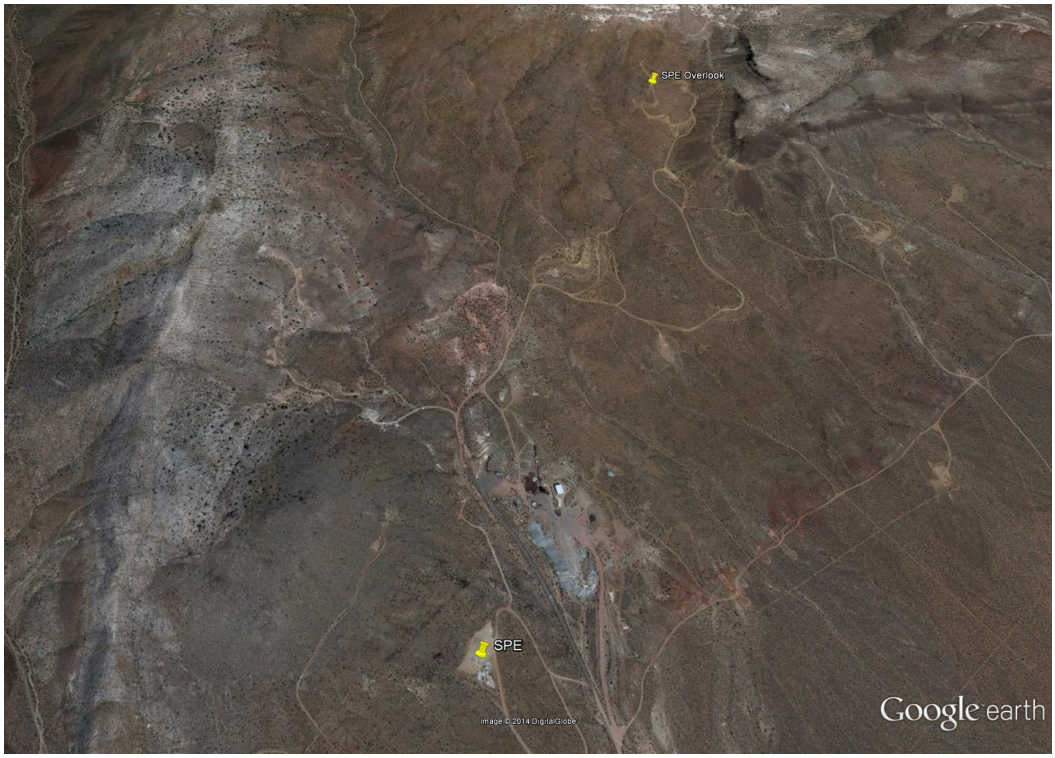

Figure 23: Google Earth® optical imagery of the SPE and its overlook.

Table 2: Table of commercial SAR collections for the NNSS bistatic SAR experiment capturing SPE IV.

Satellite	Mode	Date and Time (UTC)	Azimuth Angle (degrees)	Look Angle (degrees)	Target
CSK-4	Enhanced Spotlight	16Aug13, 00:46:10	280.94	34.53	SPE
TSX	High-Resolution Spotlight Mode	15Aug13 13:58:21	280.96	20.95	SPE

Figure 24. SPE overlook site where the base-station is inside the van on the left-side of the picture. The SPE site is the bare-earth patch in the upper right-side of the picture just to the right of the yellow drilling structure from a distant-past experiment.

Figure 25. The reflected-energy antenna was perched on a rock. A sling holding a rock stabilized the tripod assembly. The GPS antenna is the white antenna in front of the Sandian.

Figure 26. The back panel of the base station. The two gray cables are the antenna cables. The GPS antenna cable is about to be connected. The black power cord into the UPS is at the bottom of the rack with the gas power generator in the bottom left corner of the picture.

5.5. Captured Signal and SAR Imagery

Settings previously tested for the down-converter attenuation were employed for the NNSS collects. The Pentek® digitizer was set for an automatic capture of the desired TSX signal by setting the time and duration of the collection. Unfortunately, the recorder was not "armed" so the time passed without triggering the digitization of the captured signal. For the CSK collection, the Pentek® was "armed", and the signal captured.

Signal levels from the CSK collection proved to be similar to that collected at Kirtland AFB. Successful image formation was possible using PFA. The resulting side-scattering bistatic image is shown in Figure 27. This is a range-Doppler image where range is range from the reflected-energy antenna from the top of the page to the bottom, and Doppler is across the image. There are distinct differences between this image and those collected in New Mexico. There is a bright image occupying most of the image, and a faint echo of the top-most portion to the right of the bright image. This echo may be due to the pulse repetition rate of the CSK signal not being fast enough to support the image patch in the bistatic Doppler direction, thus giving aliased energy and producing a subsequent image ghost. The reflected-energy antenna is the bright point in the top, left-center of the image. Large shadows are apparent from top to bottom of the image because the reflect antenna makes a 5.5° elevation angle with the terrain around the SPE site. The sharp drop in intense along a diagonal line from the reflected-energy antenna running to the right-most lower corner is where the bistatic geometry produces no range and Doppler points on the ground, and no image can be made past this point. Figure 28 shows the geo-located CSK bistatic SAR imagery of the SPE site. The SPE site and the Sedan crater are annotated in this image. The extent of the bistatic image is approximately 8.6 km. The reflected-energy antenna site has been cropped from the picture, but is just off the top right-most corner.

Figure 29 presents a close-up of the SPE site's pad. Note the large shadows in the bistatic image on the right due to the reflect-energy antenna's low elevation angle. The reflected energy off the pad for the monostatic image is less than the bistatic. More signal level may make changes on the pad more noticeable than using the monostatic imagery.

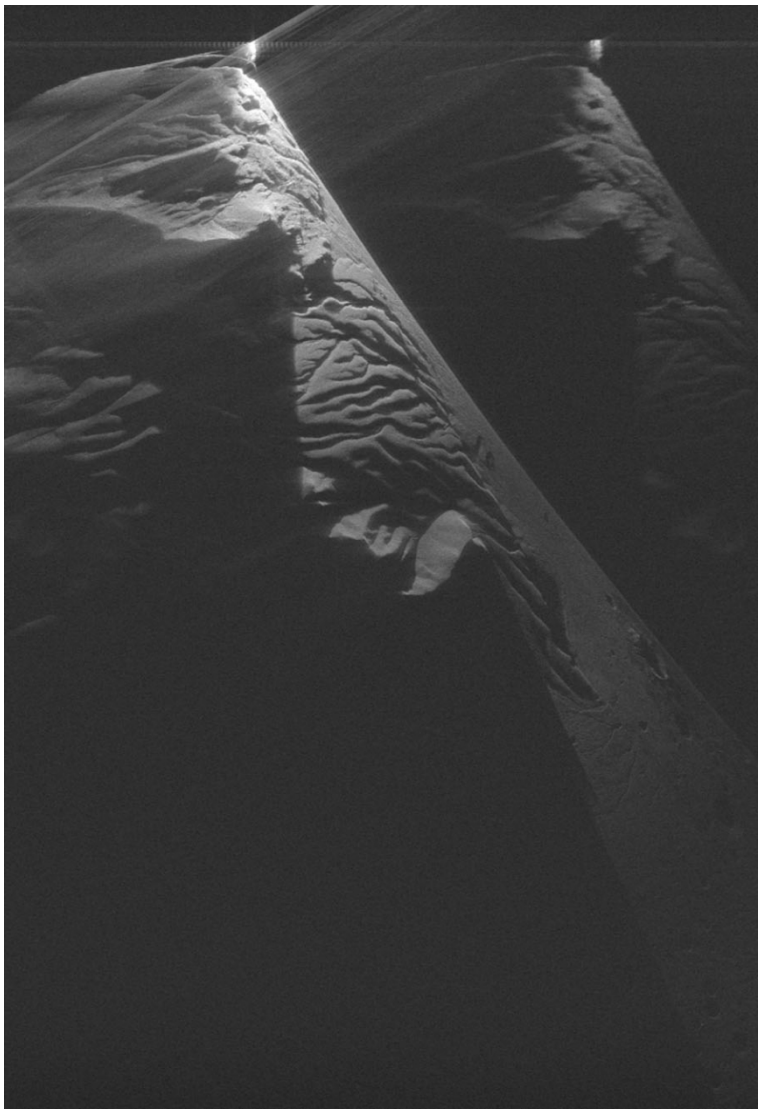

Figure 27. Bistatic SAR image created using PFA of the SPE site and its surrounding area.

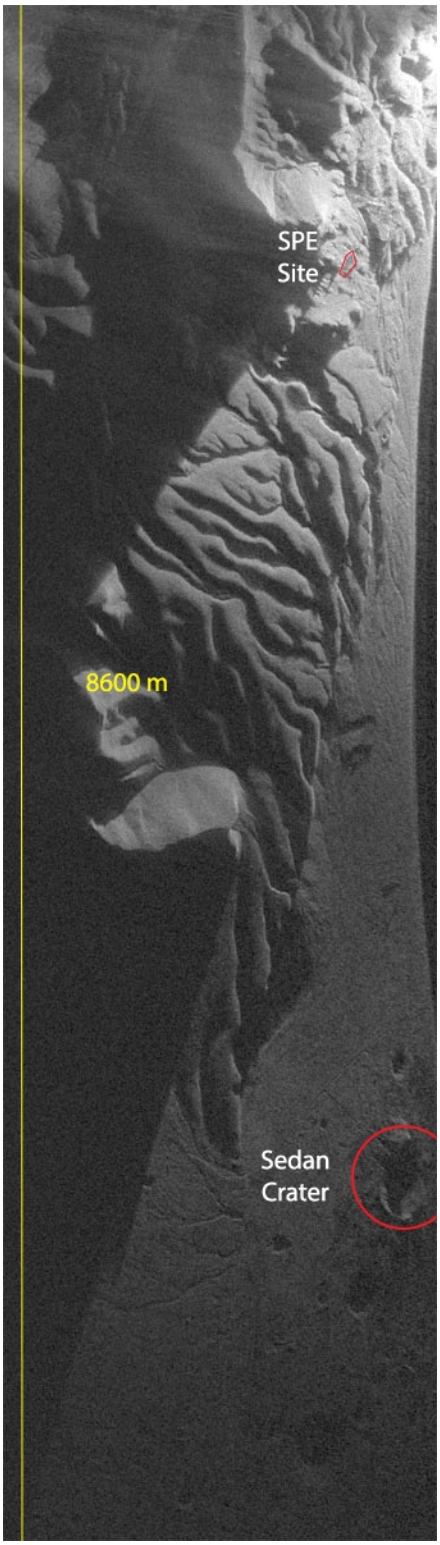

Figure 28. Geo-located bistatic SAR image of the SPE site and its surroundings. The SPE site and Sedan crater are called-out in the image.

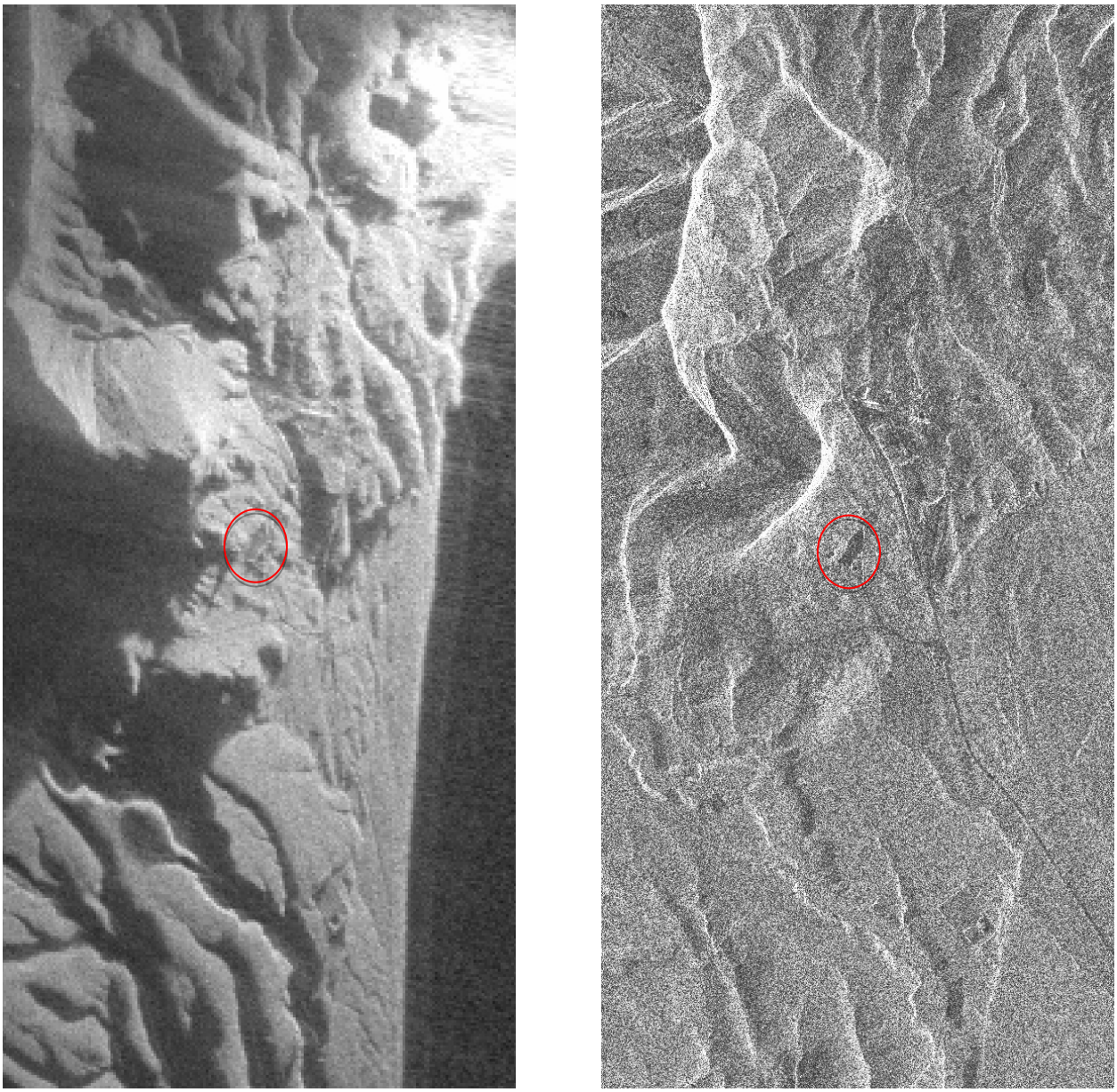

Figure 29. The left image is the bistatic image formed from captured CSK signals on August 15, 2013 at 18:46:10 PDT of the SPE pad and surrounding area. The elevation angle of the reflect-energy antenna was 5.5°. Note the long shadows due to this angle's shallowness. The right image is the monostatic CSK image. The red circle encloses the SPE pad. The SPE pad and the road to it are darker in the monostatic than the bistatic image.

6. CONCLUSION

SNL developed the means to capture spaceborne SAR signals using a ground-based system. To accomplish this, custom hardware, RADAR antennas, commercial hardware, both commercial and SNL-written software, were employed to capture, down-convert, digitize, analyze, format, and form into bistatic SAR imagery. Initial trials for hardware and experimental concept validation were conducted on Kirtland AFB utilizing commercial spaceborne SARs as the illuminating sensors. After hardware iterations and verifications, the bistatic SAR base station and accompanying antennas were transported to NNSS to capture commercial spaceborne SAR signals illuminating the SPE IV event on August 15, 2013. The hardware and software integration and utilization proved the concept of passively capturing SAR signals from a ground-based digitizing receiver using publicly available TLE files to determine the SAR sensor's position during the collection.

Images from the digitized and formatted signals were accomplished using the polar format algorithm. The images could be geo-located using the SAR ephemeris derived from the TLE files. Given these results, efforts to automate this concept are beginning.

REFERENCES

[1] C. V. Jakowatz Jr., D. E. Wahl, P. H. Eichel, D. C. Ghiglia and P. A. Thompson, Spotlight-mode Synthetic Aperture Radar: A Signal Processing Approach, Boston: Kluwer Academic Publishers, 1996.

[2] P. H. Eichel, "Fast algorithms for 3-d terrain mapping using spotlight-mode SAR stereo," in *Proceedings for the Workshop on Synthetic Aperture Radar Technology*, Huntsville, 2002.

[3] C. V. Jakowatz Jr, D. E. Wahl and D. A. Yocky, "A beamforming algorithm for bistatic SAR image formation," in *Proceedings of the SPIE: Algorithms for Synthetic Aperture Radar Imagery XVII*, Orlando, 2010.

[4] D. E. Wahl, D. A. Yocky, D. B. J. Bussey and C. V. Jakowatz Jr., "Generating lunar bistatic SAR images using Arecibo and Mini-RF," in *Proceedings of the SPIE: Algorithms for Synthetic Aperture Radar Imagery XIX*, Baltimore, 2012.

[5] R. H. Graham, D. L. Bickel and W. H. Hensley, "The rapid terrain visualization interferometric synthetic aperture radar sensor," in *Proceedings of the SPIE: Earth Observing Systems VIII*, San Diego, 2003.

[6] L. M. Wells, K. W. Sorensen, A. W. Doerry and B. L. Remund, "Developments in SAR and IFSAR systems and technologies at Sandia National Laboratories," in *IEEE Aerospace Conference Proceedings*, Big Sky, 2003.

[7] D. F. Dubbert, A. D. Sweet, G. R. Sloan and A. W. Doerry, "Results of the sub-thirty-pound, high resolution "miniSAR" demonstration," in *Proceedings of the SPIE: Conference on Airborne Intelligence, Surveillance, Reconnaissance (ISR) Systems and Applications III*, Kissimmee, 2006.

[8] K. W. Sorensen, "Advances in SAR technologies at Sandia National Laboratories," in

Proceedings of the Military Radar Conference, Washington, D.C., 2008.

[9] K. W. Sorensen, D. L. Bickel, D. W. Harmony and A. A. Martinez, "Multi-mode, fine-resolution, miniaturized Radar systems for UAVs," in *Proceedings of the IDGA Military Radar Summit*, Alexandria, 2012.

APPENDIX A: DOWN-CONVERTER BLOCK DIAGRAM

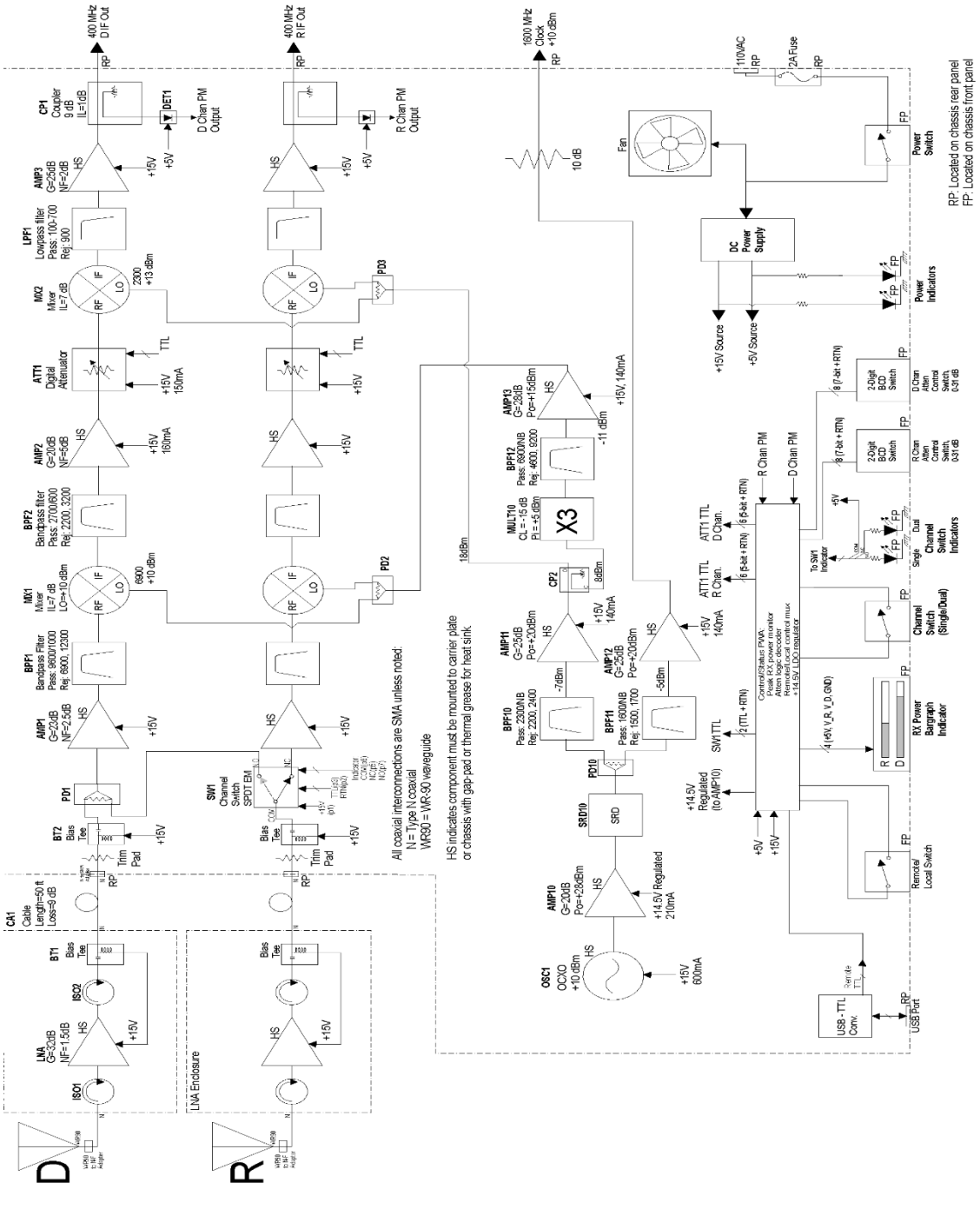

APPENDIX B: SUPPORT ACTIVITIES REQUESTED FROM NSTEC

Listed below is an explanation of the support required from NSTec, including infrastructure, equipment, services, and personnel, needed to complete the experiment.

Infrastructure, equipment, and services needs

- Vehicles (e.g. government car, van, truck, off-road truck, off-road all-terrain vehicle (ATV)).
  - Off-road vehicle to transport personnel the overlook.
  - Off-road ATV if off-road vehicle is left at the overlook.
- 120 V AC, 5 kW, 20 amp electrical generator with 4 hours of fuel.
- Photography of bistatic SAR equipment and setup at location.
- Communications: handheld radios and Wi-Fi computer communications.
- Hand-held GPS readings of bistatic antennas positions.

NSTec Personnel Needs

The basic personnel plan for the experiment is as follows:

Time Frame Relative to Experiment	Description	Type (e.g. Geologist, Engineer, RCT, etc.)	Number of Man-Days for NSTec Personnel
Aug. 5 – Aug. 9	NSTec Coordinator		1
August 14	Support team	Technician	0.5
August 15	Support team/driver	Technician	0.5

DISTRIBUTION

1 Veraun Chipman
NCNS/CIT Program Manager
National Security Technologies (NSTec)
PO Box 98521
M/S NLV101
Las Vegas, NV 89193-8521

1	MS0532	Gilbert G. Delaplain	5344
1	MS0532	William H. Hensley, Jr.	5344
1	MS0532	Bertice L. Tise	5348
1	MS0532	Thomas J. Trodden	5348
1	MS0533	Dale F. Dubbert	5345
1	MS0533	Kurt W. Sorensen	5345
1	MS0971	Robert M. Huelskamp	5750
1	MS1205	Ann. N. Campbell	5900
1	MS1207	Terry A. Bacon	5962
1	MS1207	Neall E. Doren	5962
1	MS1207	Charles V. Jakowatz, Jr.	5962
1	MS1207	Daniel E. Wahl	5962
4	MS1207	David A. Yocky	5962
1	MS1209	John E. Gronager	5960
1	MS0899	Technical Library	9536 (electronic copy)


Sandia National Laboratories